# Viscoelastic Properties of Poly(styrene-*co*-acrylate) and Poly(vinylcyclohexane-*co*-acrylate) Ionomers

**Joon-Seop Kim, Gaoming Wu,† and Adi Eisenberg***

*Department of Chemistry, McGill University, 801 Sherbrooke Street West, Montreal, Quebec, Canada H3A 2K6*

*Received August 26, 1993; Revised Manuscript Received November 1, 1993*®

ABSTRACT: To investigate the effect of the chemical structure of the copolymers on the mechanical properties and morphology of ionomeric materials, two different series of acrylate ionomers were synthesized, i.e., poly(styrene-*co*-acrylate) and poly(vinylcyclohexane-*co*-acrylate) ionomers. Even though the general trends of the mechanical properties of the styrene–acrylate copolymers are similar to those of the styrene–methacrylates, there are some differences. For the methacrylates, the contact surface area of the chain is bigger due to the presence of the methyl group, and thus the multiplets in the methacrylate ionomers are smaller than those in the acrylates. Therefore, the glass transition temperature of the clusters is higher, and the ionic plateau is also higher and longer for the methacrylates than the acrylates. This is also consistent with the small-angle X-ray scattering (SAXS) results which show that the Bragg spacing in the methacrylates is marginally smaller than that in the acrylates. For the vinylcyclohexane ionomers, thermogravimetric analysis (TGA) shows that these are thermally stable up to 310–340 °C depending on the ion content. In this system, both the matrix and the cluster $T_g$s are higher than those in the styrene-based ionomers. This behavior arises from the bulkiness of the pendant group, i.e., cyclohexyl, which increases the stiffness of the chain relative to that of styrene. For all the systems studied here, with increasing ion content, the matrix $T_g$ increases in parallel with the cluster $T_g$. This is reasonable because the material in both phases is based on the same polymer. Differential scanning calorimetry (DSC) thermograms show only one glass transition curve for all the systems, corresponding either to the matrix or to the cluster $T_g$ depending on which one is dominant. The $T_g$s obtained from the DSC are identical with those determined from loss modulus peak maxima at 0.3 Hz.

## Introduction

During the past 2 decades, the mechanical properties and morphologies of random ionomers have been studied extensively.[1-11] A number of models were proposed to explain the morphologies and mechanical properties of these materials in the solid state.[7,8] There is a generally acceptable concept that ion pairs aggregate to form multiplets.[12] Recently, Eisenberg, Hird, and Moore (EHM) proposed a new morphological model for random ionomers.[13] They argue that the multiplets cause a restriction of the mobility of the polymer segments adjacent to the multiplet. With increasing ion content, the partially immobilized regions begin to overlap. Eventually, when the ion content is high enough, the immobilized regions begin to form sufficiently large domains, the so-called "cluster", in which the material exhibits phase-separated behavior, including a second glass transition at a higher temperature than that of the matrix. At low ion contents, the regions of unrestricted mobility dominate; at high ion contents, the restricted mobility regions become dominant. This model reconciles a wide range of phenomena in the random ionomers, especially in terms of relating molecular parameters to two-phase behavior.

Extensive studies have shown that a large number of parameters are important in the formation of multiplets and clusters in random ionomers, e.g., the ion content, the size of ionic group, the type of counterion, the dielectric constant of the polymer backbone, the position of the pendant ion, the amount and nature of plasticizer, etc. However, very few studies have compared ionomers having an identical backbone and ion content but different acid groups. Some examples are the work of Lundberg and Makowski,[14] Rigdahl and Eisenberg,[15] Visser and Cooper,[16] and Venkateshwaran et al.[17] These studies compared sodium-neutralized carboxylated and sulfonated ionomers and showed that the sulfonated ionomers lead to stronger aggregates than the analogous carboxylates which results, among others, in increased moduli and viscosities for the sulfonates at comparable temperature.

MacKnight et al.[18-21] published a series of studies on the carboxylated, phosphonated, and sulfonated polypentenamer ionomers. However, extensive conclusions about the influence of the types of pendant ionic groups on the properties of the ionomers are not easily reached because the detailed synthetic methods for these ionomers were different and because properties of the ionomers are affected significantly by the degree of crystallinity, crosslinking, and the molecular weight of the materials.[16]

Hird and Eisenberg[22] investigated the effect of the type of cations on the mechanical properties of alkali-metal-neutralized poly(styrene-*co*-methacrylate) [P(S-*co*-MA)] ionomers and found that $Na^+$-, $Li^+$-, and $Rb^+$-neutralized P(S-*co*-MA) show similar apparent activation energies for the matrix and cluster glass transitions. In a subsequent study, the mechanical properties of the carboxylated and sulfonated styrene ionomers, i.e., P(S-*co*-MA), carboxylated polystyrene [P(S-*co*-CS)], and sulfonated polystyrene [P(S-*co*-SS)], were investigated by Hird and Eisenberg[23] in order to determine the effects of the type of the anionic groups and their positions relative to the polymer backbone. They found that the ionic moduli of the materials are different from each other, and they suggested that these differences are due to the differences in the sizes and stabilities of multiplets. Also, they found that the position of the ion pairs relative to the polymer backbone exerted an influence on the mechanical properties of the ionomers. The effects of the position of the ions on mechanical properties and morphologies of the styrene ionomers were discussed in much greater detail by Gauthier and Eisenberg and Moore et al. Gauthier and Eisenberg studied the effect of the various lengths of

---

* To whom all correspondence should be addressed.

† Present address: Neste Resins Canada, 1919 Wilson Ave., Weston, Ontario, Canada M9M 1B1.

® Abstract published in *Advance ACS Abstracts*, December 15, 1993.

0024-9297/94/2227-0814$04.50/0

side chain on the dynamic mechanical properties of carboxylated styrene ionomers [P(S-*co*-C$_n$–ether) or P(S-*co*-C$_n$–alkyl)].[24] The importance of three distinct factors was suggested, i.e., the bulkiness and rigidity of the units to which the pendant ionic groups are attached, the immobilizing effect of the ionic groups on the polymer backbone, and the presence of the solvating ether linkage. Also a small-angle X-ray scattering (SAXS) study of the random styrene ionomers with variable-length side chains by Moore et al.[25] showed that increasing the distance of the ionic groups from the polymer backbone leads to larger multiplets and a greater intermultiplet spacing. This arises from the reduced steric hindrance to formation of aggregates as the distance of the ions from the backbone is increased.

Clas and Eisenberg[26] investigated the mechanical properties of sodium-neutralized poly(styrene-*co*-4-hydroxystyrene) and poly[styrene-*co*-4-(hydroxymethyl)styrene] and compared the results with those of other styrene ionomers. They showed that the glass transition temperature of the matrix, the size of multiplets, and the strengths of the ionic interactions were related to the type and position of their ionic groups.

There are a number of studies of different ionomer families which explore their structures and properties. For instance, there are many studies on the styrene-based ionomers,[3,5,6] the ethylene-based ionomers (e.g., Surlyn),[27] and the perfluorinated ionomers (e.g., Nafion),[28] etc. As was mentioned before, some of the studies on these ionomers have addressed themselves to the elucidation of the parameters which are of importance in influencing the formation of multiplets and clusters. However, even though there are many studies on these materials, much less attention has been devoted to the systematic variation of the parent polymer. When one explores the effect of the structure of the main chain on the properties of ionomers, there are many variables to be considered, e.g., the differences in the molecular weight, the molecular weight distribution, crystallinity, sequence distribution of the ionic units along the backbone chain, etc. Thus, it is not easy to compare the properties of ionomers which are obtained from different ionomer families. Since the purpose of this study is to make direct comparisons between materials obtained from different ionomer families, the materials were selected so as to minimize the number of the parameters which change from family to family.

In the present study, we explore two parameters, specifically the effect of changing the benzene ring of the styrene to a cyclohexyl group and also the effect of replacing the methyl group on the backbone carbon atom in methacrylic acid with hydrogen, i.e., the effect of replacing methacrylic acid with acrylic acid. Thus, taking poly(styrene-*co*-acrylate) ionomer [P(S-*co*-AA)] as a reference system, comparison will be made, on the one hand, between P(S-*co*-AA) and poly(vinylcyclohexane-*co*-acrylate) [P(VCH-*co*-AA)] ionomers and, on the other hand, between P(S-*co*-AA) and poly(styrene-*co*-methacrylate) [P(S-*co*-MA)] ionomers. The mechanical properties of the P(S-*co*-MA) ionomers have been reinvestigated very recently in great detail, and thus comparisons could be made with the results obtained in that study. In addition, the difference in the mechanical properties of the cesium- and sodium-neutralized P(S-*co*-AA) ionomers is addressed briefly.

## Experimental Section

**Synthesis and Characterization. (1) Poly(styrene-*co*-acrylic acid) [P(S-*co*-AA)] Random Copolymers.** Styrene (Aldrich, 99%) and acrylic acid (Aldrich, 99%) were purified by fractional distillation at 47 °C (21–22 mmHg) and 39–40 °C (15 mmHg), respectively. The distilled monomers were stored in a freezer at −20 °C prior to use. Benzoyl peroxide (Aldrich, 97%) was used as received.

The random copolymers were prepared by free-radical bulk copolymerization of styrene and acrylic acid using benzoyl peroxide as initiator. The reactivity ratios used for the calculation of the initial compositions of the copolymers are 0.35 for acrylic acid and 0.22 for styrene.[29] The percentage conversion was 8–20%, yielding a compositional heterogeneity of less than 0.35.

The copolymerization was carried out in a flask equipped with a ground-glass stopcock. The two monomers and the initiator were mixed in a reaction flask and degassed by three cycles of freezing–evacuating–thawing. The flask was then immersed in a water bath for 3.5–5 h at 60 °C, to achieve a conversion ranging from 8 to 20%. The reaction mixture was then cooled and diluted with 20 volumes of tetrahydrofuran (THF). The polymer sample was recovered by precipitation into a rapidly stirred excess of a methanol/water mixture (80/20, v/v). The stirring was continued for a few hours to extract the monomers out of the polymer. The precipitated polymer was then filtered, immersed into a fresh methanol/water mixture, stirred overnight, filtered again, and dried under vacuum at 60 °C for at least 2 days. To determine the acid concentration, samples were dissolved in a benzene/methanol (90/10, v/v) mixture to make a 5% (w/v) solution and titrated to the phenolphthalein end point with standard methanolic sodium hydroxide. While the molecular weights of the polymers were not measured directly, for the copolymerization calculated amounts of initiator were added to obtain a molecular weight in the range of 100 000. It should be mentioned that, as a part of another project,[30] a series of P(S-*co*-MAA) samples was prepared in the same way, except for the amounts of initiator. For the methacrylates, the calculated amounts of initiator were added to obtain the molecular weight of ca. 500 000. The molecular weights were subsequently determined for that system using size-exclusion chromatography. The results showed that in that series the molecular weights were, indeed, in the range of 400 000–600 000. This is discussed in great detail elsewhere.[30] From these results, one can see that the molecular weights of the P(S-*co*-AA) ionomers should be in the range of ca. 100 000.

**(2) Poly(vinylcyclohexane-*co*-acrylic acid) [P(VCH-*co*-AA)] Random Copolymers.** Since the hydrogenation procedure is accompanied by the reduction of carboxylic acid to the corresponding alcohol, methyl acrylate was used as a comonomer instead of acrylic acid.

**(a) Copolymerization of Styrene and Methyl Acrylate.** Styrene (Aldrich, 99%) was purified as described above. Methyl acrylate (Aldrich, 99%) was distilled at ambient temperature (50 mmHg). The distilled monomers were stored in a freezer at −20 °C until use (within 3 days). Benzoyl peroxide (Aldrich, 97%) was used as received.

The random copolymers were synthesized by bulk copolymerization of the monomers initiated with benzoyl peroxide. The reactivity ratios used for the calculation of the initial composition of the copolymers are 0.18 for methyl acrylate and 0.75 for styrene.[29] The conversion was 10–30%, yielding a compositional heterogeneity of less than 0.1.

The copolymerization was carried out in a flask equipped with a ground-glass stopcock. A series of mixtures of the monomers with different monomer ratios were prepared to obtain copolymers with methyl acrylate contents of 2–21 mol %. The monomers and initiator were mixed in a reaction flask and degassed by three cycles of freezing–evacuating–thawing. The amounts of initiator were calculated to obtain a molecular weight in the range of 100 000. The flask was then immersed in a water bath for ca. 9 h, at 60 °C, to achieve a conversion ranging from 10 to 30%. The polymer solution was diluted with 20 volumes of THF and then precipitated into rapidly stirring methanol. The stirring was continued for a few hours to extract more monomers out of the polymer. Finally, the precipitated polymer was filtered, washed with fresh methanol, filtered again, and then dried in a vacuum oven at 60 °C for 2 days. The methyl acrylate content of the polymer was calculated from the relative intensities of the NMR peaks of the methyl protons at 3.2 ppm and the aromatic protons at 6.0–7.8 ppm.

**(b) Hydrogenation of Poly(styrene-*co*-methyl acrylate).** The copolymers of styrene and methyl acrylate were hydrogenated using a modification of Osada's method.[31] Silica/alumina-supported nickel with a surface area of 190 $m^2/g$ (Aldrich) was used as the catalyst. For a typical hydrogenation, the copolymer was dissolved in a mixture of cyclohexane and ethyl acetate (60/40, v/v) in a glass tube, and then silica/alumina-supported nickel was added. The tube was placed in a high-pressure reactor, and the mechanical stirrer, heating mantle, and hydrogen line were assembled. While the solution was being stirred vigorously, the air in the reaction system was removed by purging with $H_2$ for 2 min. The $H_2$ pressure was then increased to 10 MPa, and the system was closed and heated to 180 °C. The stirring was continued for 20 h at that temperature, the hydrogenation was terminated, and the reactor was allowed to cool to room temperature. The reaction mixture was diluted with 3 volumes of THF and passed through an alumina column to remove the Ni particles. The volume of solution was reduced by evaporation to about $^1/_3$ of the total volume, and then the polymer was recovered by precipitation into rapidly stirring methanol. After stirring overnight, the copolymer was filtered, washed with fresh methanol, and dried under vacuum at 60 °C for 2 days. The decrease of the intensities in the NMR peaks of aromatic protons in the range of 6.0–7.8 ppm indicated that more than 90% of the benzene rings in the copolymer had been hydrogenated.

**(c) Hydrolysis of Poly(vinylcyclohexane-*co*-methyl acrylate).** The methyl acrylate groups were hydrolyzed by refluxing in a KOH/THF/methanol/$H_2O$ mixture under a nitrogen atmosphere. For a typical hydrolysis, 5.8 g of poly(vinylcyclohexane-*co*-methyl acrylate) (21.5 mol % of methyl acrylate) was dissolved in 200 mL of THF, and 30 mL of a 5 M KOH solution in a methanol/water (90/10, v/v) mixture was added slowly to the polymer solution under vigorous stirring. The polymer solution became somewhat cloudy but cleared upon the gradual addition of methanol (50 mL). Refluxing of the solution was continued for 5 days. Once the refluxing was stopped, the polymer was precipitated by the addition of about 500 mL of distilled water. After decantation of the solvent, the polymer was washed with water several times, followed by washing with methanol. The polymer was then dissolved in 200 mL of a THF/methanol (90/10, v/v) mixture. Concentrated hydrochloric acid was dropped into the stirring solution until the pH was well below 2. After stirring for 4 h, distilled water (500 mL) was added. The solution was stirring for a few additional hours, and then the volume of solvent was reduced to cause the polymer to precipitate. The solvent was decanted, and the polymer was washed with water a few times. It was filtered, dried in a vacuum oven at 70 °C overnight, and dissolved in 100 mL of a benzene/methanol (85/15, v/v) mixture. Finally, it was precipitated into rapidly stirring methanol, and the precipitate was stirred overnight, filtered, washed with methanol, and dried in a vacuum oven at 60 °C for 2 days. The completion of the hydrolysis was confirmed by the complete disappearance of the proton NMR peaks of the methyl ester groups. To determine the acid concentration, the same procedure was used as for the styrene-*co*-acrylic acid samples.

**Sample Preparation.** The P(S-*co*-AA) samples were dissolved in a benzene/methanol (90/10, v/v) mixture to give a 5% (w/v) solution. To neutralize the acrylic acid groups, a predetermined quantity of methanolic sodium hydroxide was added to give poly(styrene-*co*-sodium acrylate) [P(S-*co*-AANa)]. The solutions were freeze dried and then dried under vacuum at 160 °C for at least 1 day. The cesium-neutralized ionomer was prepared in the same way as the sodium-neutralized samples. The P(VCH-*co*-AA) samples were neutralized in the same way as the P(S-*co*-AA) ionomers. The sample notation used for the ionomers is P(S-*x*-AA*y*) for the styrene-*co*-acrylate ionomers and P(VCH-*x*-AA*y*) for vinylcyclohexane-*co*-acrylate ionomers, where *x* is the mole percent of the acrylate and *y* is the type of cation.

For the dynamic mechanical thermal analysis (DMTA) measurements, samples were compression molded at 240 °C under a pressure of ca. 20 MPa. The pressure was applied for 5 min; then it was slowly released, and the mold was slowly cooled to below the matrix $T_g$. The sample was removed from the mold and annealed for 24 h under vacuum at around 220 °C. The dimensions of the molded sample were ca. 2.5 × 6.0 × 30.0 mm.

For the SAXS studies, the cesium-neutralized samples were compression molded at 220 °C under a pressure of ca. 20 MPa. The molded samples in the form of a thin disk with dimensions of 12 mm (diameter) × 0.6 mm (thickness) were stored under vacuum at 100 °C for 24 h.

For the differential scanning calorimetry (DSC) measurements, ionomers in powder form were further dried at 220 °C under vacuum for 1 day and cooled to below the matrix glass transition temperature, i.e., ~100 °C during a period of 2 min.

**Dynamic Mechanical Thermal Analysis (DMTA).** Dynamic mechanical property measurements were performed on a Polymer Laboratories dynamic mechanical thermal analyzer (DMTA). Storage moduli ($E'$), loss moduli ($E''$), and loss tangents (tan $\delta$) were obtained as a function of temperature at a heating rate of 0.5 °C/min. The experiments were performed in the dual cantilever bending mode at frequencies ranging from 0.3 to 30 Hz. All experiments were carried out under a dry nitrogen atmosphere.

**Small-Angle X-ray Scattering (SAXS).** The small-angle X-ray scattering experiments for the P(S-*co*-AACs) systems were conducted at station D-22 of the LURE-DCI synchrotron radiation source (Orsay, France). A fixed-exit, double-crystal monochromator was used to provide a beam of 9.0-keV X-rays ($\lambda$ = 1.38 Å). The size of the beam at the sample was smaller than 1 $mm^2$. The detectors, which consisted of two beam deflectors and a NaI scintillator, were positioned before and after the sample chamber to monitor the relative input X-ray intensity and the sample absorption. A Xe–$CH_4$ gas-filled, one-dimensional position-sensitive detector with a resolution of 200 $\mu$m was used to detect the scattered X-rays. The sample-to-detector distance of 597 mm allowed SAXS data to be obtained in the $q$ range from 0.018 to 0.37 $Å^{-1}$. The SAXS data were plotted as relative intensity vs $q$ after correction for background scattering (the SAXS profile of pure polystyrene was subtracted from that of each ionomer samples) and sample absorption. All samples were normalized to a thickness of 1 mm.

For the SAXS studies for the P(VCH-*co*-AACs) samples, a Warhus SAXS camera at the Pulp and Paper Research Institute (Paprican) was used. X-ray diffraction patterns were recorded on a flat film. Ni-filtered Cu K$\alpha$ radiation ($\lambda$ = 1.548 Å) was utilized. The X-ray beam was generated by a Philips PW 1730 X-ray generator (40 kV and 20 mA). The diameter of the hole of the collimator was 0.015 in., and the sample-to-film distance was 160 mm. Each experiment was performed under vacuum for 16 h.

**Differential Scanning Calorimetry (DSC).** For the thermal analysis studies, a Seiko differential scanning calorimeter (DSC 220) was used. It was calibrated with indium. The sample cells, which contained around 4–10 mg of ionomer, were stored under a dry ntirogen atmosphere, the flow rate of which was 50 mL/min. To ensure a uniform thermal history, the ionomers were first scanned at 20 °C/min up to the range of 150–290 °C depending on the ion concentration and held at that temperature for 30 min; they were then allowed to cool to below the matrix $T_g$ during a period of 15–30 min. The samples were scanned again from 80 °C to above the second glass transition temperature, i.e., 150–320 °C, to span the range of the two glass transition temperatures. The glass transition temperatures were taken as the midpoint of the heat capacity plot between two base lines.

**Thermogravimetric Analysis (TGA).** For the studies of the thermal stability of ionomers, a Seiko thermogravimetric/differential thermal analyzer (TG/DTA 220) was used. The experiments were performed as a function of temperature, over the range of 50–500 °C at a heating rate of 20 °C/min under dry nitrogen at a flow rate of 250 mL/min.

**Data Analysis.** For each sample, dynamic mechanical property measurements were performed at five different frequencies; however, detailed analysis was performed only on the 1-Hz data. Curve resolutions were performed on the loss tangent data using the Peakfit (Jandel Scientific) program. The best fits were achieved by using the WLF relation as a background and fitting the matrix and cluster peaks with exponentially modified Gaussian functions. The equations for the fitting curves are described elsewhere.[30] Curve resolutions were carried out over the temperature range from 100 to approximately 20 °C above the minimum following the cluster peak.

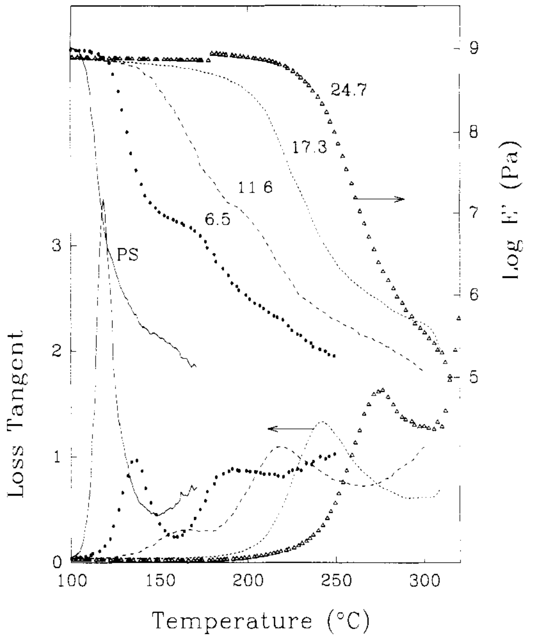

**Figure 1.** Storage moduli ($E'$) and loss tangents (tan $\delta$) measured as a function of temperature at 1 Hz for polystyrene and several P(S-*co*-AANa) ionomers. The molar ion content is indicated for each sample.

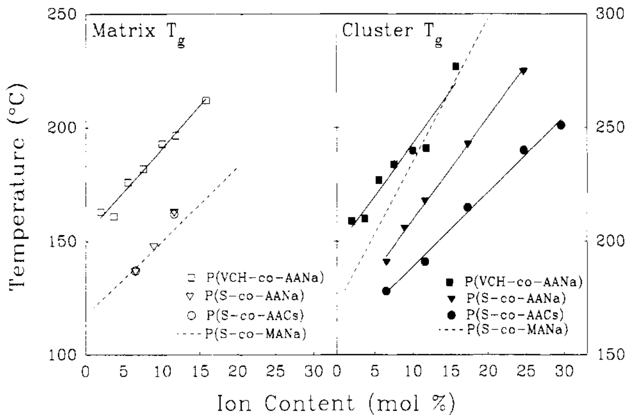

**Figure 2.** Loss tangent peak positions measured at 1 Hz for the ionomers. Open symbols indicate the matrix $T_g$ peaks; filled symbols indicate cluster $T_g$s.

Activation energies for the matrix and cluster transitions were calculated using an Arrhenius plot of log frequency vs inverse peak temperature. The standard deviation in the slope was used as an estimate of the error in the slope.

## Results and Discussion

**P(S-*co*-AA) Ionomers.** Figure 1 shows the plot of a series of storage modulus and loss tangent curves for P(S-*co*-AANa) ionomers of various ion contents as a function of temperature. The loss tangent curves for the 6.5 and 11.6 mol % ionomers show two glass transition peaks. The first peak is associated with the glass transition of the matrix, while the second reflects the glass transition of the cluster regions.[22] As expected, both glass transition temperatures increase with increasing ion content. The peak temperatures are plotted in Figure 2, along with those for other systems determined from the present work or from previous studies in this laboratory. For the Cs-neutralized samples above ca. 11 mol % of ions, no independent peak due to the matrix phase can be seen. This is probably due to the fact that the volume fraction of the matrix phase is now very small, and the matrix peak overlaps with the cluster peak. However, curve resolution still allows it to be detected. The curve resolution results are listed in Table 1 along with those for the other samples. As for other ionomers,[22,30] the area under the matrix peak for this system decreases with increasing ion content, while that for the cluster peak increases. The width at half-height of the matrix peak increases, while that for the cluster peak decreases with increasing ion content. The peak width is probably related to phase homogeneity; this will be discussed in detail in another publication.[30] Similar plots for the P(S-*co*-AACs) ionomers were obtained but are not shown here; the results, however, are also given in Table 1. It should be noted that the points shown in Figure 2 are the actual maxima obtained from the plots, while the values in Table 1 are those obtained from the curve resolution procedure.

The storage modulus curves in the transition region for the materials at the compositional extremes show a high degree of similarity, which is illustrated in Figure 3. That figure compares the storage moduli of polystyrene and of the P(S-29.6-AACs) ionomer as a function of temperature. It should be mentioned that to facilitate the comparison the curve for the ionomer was shifted to lower temperatures, with the label of the temperature axis for the ionomer indicated at the top of the plot. The slope of the log $E'$ vs temperature curve of polystyrene in the transition range is very steep; it should be recalled that this transition is due to the glass transition of the "matrix" only, since, obviously, no cluster material is present in pure polystyrene. The slope for the P(S-29.6-AACs) plot is also very steep, with a shape which is very similar to that of the polystyrene. However, it should be stressed that this transition is associated with the glass transition of the "cluster" regions only, since no trace of a "matrix peak" is visible in the tan $\delta$ plot. Polystyrene shows only one-phase behavior, i.e., due to the unclustered phase, but so does the P(S-29.6-AACs) ionomer for the clustered phase. This behavior confirms the two-phase nature of partly clustered ionomeric materials by showing that very similar phenomena are seen at the compositional extremes, where only one phase is present but where the nature of that phase is very different in the two cases. For the P(S-29.6-AANa) sample, the cluster $T_g$ is much higher than that for the cesium sample, so the material was difficult to mold and the analysis of the results was very risky. Therefore, instead of the sodium sample, the modulus of the cesium sample was compared with that of polystyrene. However, the trend can also be seen when one compares the polystyrene plot with that for the P(S-24.7-AANa) in Figure 1.

The matrix glass transitions of both the sodium-neutralized and the cesium-neutralized ionomers are almost the same over the entire accessible range (0–12 mol %). The sodium-neutralized ionomers show a more extended ionic plateau, which is probably due to the stronger interaction between sodium–carboxylate ion pairs than in the cesium system. It should be mentioned, however, that one of the neutralizing agents, i.e., cesium hydroxide, was in the form of a monohydrate. The temperature for the dehydration of this monohydrate under vacuum is ca. 400 °C, and this dehydration was not performed for this study; for the sodium hydroxide, a relatively low temperature is enough to remove the water.[32–34] Therefore, it is possible that the cesium-neutralized ionomers may contain a marginally higher moisture content than the sodium-neutralized samples, even though both were dried under the same conditions. If this were the case, the water molecules would act as an external ionic-domain plasticizer and lower the cluster $T_g$

**Table 1. Loss Tangent Peak Parameters Obtained by Deconvolution for Various Ionomer Systems**

| | matrix peak | | | | cluster peak | | | | |
|---|---|---|---|---|---|---|---|---|---|
| sample | $T_{g,m}$ (°C) | width at half-height (°C) | area (°C) | % area | $T_{g,c}$ (°C) | width at half-height (°C) | area (°C) | % area | total area (°C) |
| polystyrene | 119 | 12 | 44 | 100 | | | | | 44 |
| P(S-6.5-AA) | 127 | 12 | 37 | 100 | | | | | 37 |
| P(S-6.5-AANa) | 136 | 19 | 18 | 40 | 191 | 42 | 27 | 60 | 45 |
| P(S-8.9-AANa) | 148 | 23 | 11 | 24 | 206 | 43 | 35 | 76 | 46 |
| P(S-11.6-AANa) | 162 | 32 | 7 | 15 | 218 | 46 | 41 | 85 | 41 |
| P(S-17.3-AANa) | | | | | 242 | 41 | 50 | 100 | 50 |
| P(S-24.7-AANa) | | | | | 274 | 39 | 48 | 100 | 48 |
| | | | | | | | average total area[a] | | 47 ● 2 |
| P(S-6.5-AACs) | 138 | 18 | 18 | 38 | 178 | 38 | 29 | 62 | 47 |
| P(S-11.6-AACs) | 162 | 27 | 11 | 22 | 189 | 37 | 40 | 78 | 51 |
| P(S-17.3-AACs) | | | | | 214 | 36 | 49 | 100 | 49 |
| P(S-24.7-AACs) | | | | | 241 | 27 | 49 | 100 | 49 |
| P(S-29.6-AACs) | | | | | 251 | 27 | 48 | 100 | 48 |
| | | | | | | | average total area[a] | | 48 ± 3 |
| P(VCH-2.0-AA) | 158 | 25 | 60 | 100 | | | | | 60 |
| P(VCH-2.0-AANa) | 163 | 26 | 45 | 90 | 209 | 24 | 5 | 10 | 50 |
| P(VCH-3.7-AANa) | 162 | 25 | 38 | 79 | 210 | 28 | 10 | 21 | 48 |
| P(VCH-5.5-AANa) | 176 | 36 | 37 | 76 | 226 | 39 | 12 | 24 | 49 |
| P(VCH-7.5-AANa) | 182 | 38 | 30 | 65 | 237 | 43 | 16 | 35 | 46 |
| P(VCH-10.0-AANa) | 192 | 28 | 11 | 23 | 239 | 55 | 37 | 77 | 48 |
| P(VCH-11.8-AANa) | 196 | 29 | 9 | 20 | 243 | 49 | 35 | 80 | 44 |
| P(VCH-15.7-AANa) | 211 | 36 | 6 | 13 | 276 | 50 | 39 | 87 | 45 |
| | | | | | | | average total area[a] | | 47 ± 2 |
| P(S-6.6-MANa)[b] | 139 | 20 | 13 | 30 | 208 | 47 | 31 | 70 | 44 |
| P(S-11.5-MANa)[b] | 155 | 27 | 3 | 7 | 240 | 40 | 40 | 93 | 43 |
| | | | | | | | average total area[b] | | 47 ± 2 |

[a] Data calculated from the total areas of the alkali-metal-neutralized ionomers. [b] Data obtained from ref 30.

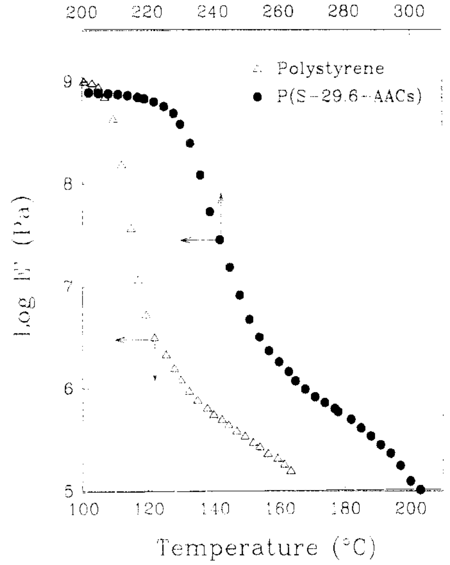

**Figure 3.** Storage modulus ($E'$) as a function of temperature for polystyrene (△) and P(S-29.6-AACs) (●). The label for the temperature axis for the indicated at the top of the plot.

by that mechanism also. This possibility cannot be ignored.

Figure 4 shows the apparent activation energies of the glass transition of the matrix and cluster regions, along with those for the other ionomers. Above 12 mol % of ions, the matrix values seem to level off, while the cluster activation energies at high ion contents approach those of the matrix or of pure polystyrene. This trend parallels that observed by Hird and Eisenberg for the P(S-*co*-MANa) ionomers at low ion contents.[22]

**Comparison P(S-*co*-AANa) Ionomers with P(S-*co*-MANa) Ionomers.** Figure 5a compares the loss tangent and the storage modulus curves for the P(S-6.5-AANa) sample with those for the P(S-6.6-MANa) sample, and

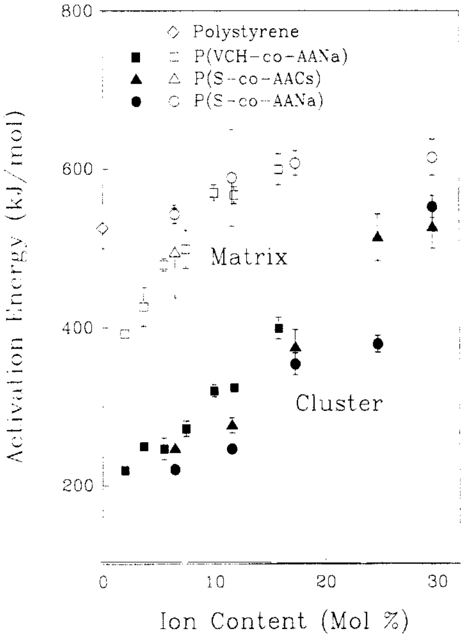

**Figure 4.** Apparent activation energies for the polystyrene (◇), (P(S-*co*-AA) (▲, ○), and P(VCH-*co*-AA) (□) ionomers as a function of ion content. Open symbols indicate the activation energies for the matrix phase, and filled symbols indicate the activation energies for the cluster phase. The error bars are derived from the standard error of the slope in the Arrhenius plot.

Figure 5b compares those for the P(S-11.6-AANa) with those for the P(S-11.4-MANa) sample. That figure also shows the results for the P(VCH-11.8-AANa) which will be discussed below. The loss tangent plots show that there are two peaks for both systems. The peak positions of the matrix glass transition for the samples which have an almost identical ion content are almost the same. Hird and Eisenberg[23] observed that the matrix $T_g$s of the polystyrene-based sulfonate [P(S-*co*-SS)], carboxylate

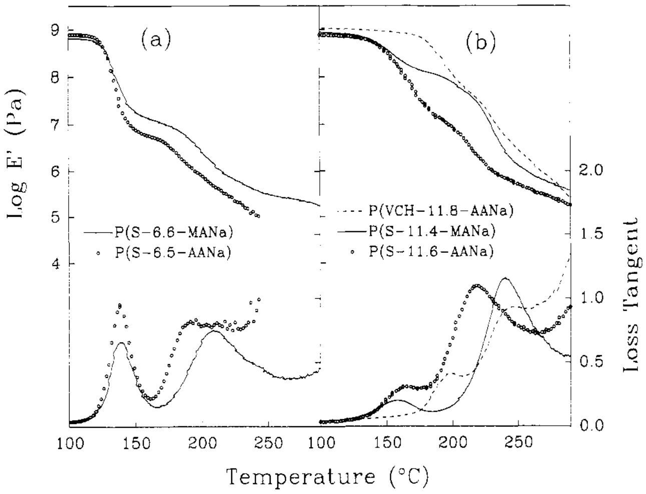

**Figure 5.** Storage modulus ($E'$) and loss tangent ($\tan\delta$) data measured as a function of temperature at 1 Hz for (a) P(S-6.6-MANa) (—) and P(S-6.5-AANa) (○) samples and (b) P(VCH-11.8-AANa) (- - -), P(S-11.6-AANa) (○), and P(S-11.4-MANa) (—) samples.

[P(S-*co*-SC)], and methacrylate [P(S-*co*-MA)] ionomers are independent of the nature of chemical structures and the types of cations but depend only on the ion content. In this study, it is also found that the matrix $T_g$s of the acrylate and methacrylate ionomers are independent of their chemical structure of the ionic comonomers or the types of cations. In the methacrylate system, however, the cluster peak maximum appears at a higher temperature than that for the acrylate ionomer. In the plot of storage modulus against temperature, the ionic plateau for the acrylates is lower and shorter than that for the methacrylates.

The ratio of the area under the cluster peak to the total area under the peaks (at high ion content, there is only one peak due to the cluster transition) for the methacrylate system is higher than that for acrylates at the same ion content, as can be seen in Table 1. For instance, the fractional areas under the cluster peak for the acrylate system are 0.60 for 6.5 mol % and 0.85 for 11.6 mol %, while those for the methacrylate ionomers are 0.70 for 6.6 mol % and 0.93 and 11.5 mol %. It should be mentioned that the average total area under the peaks for the different ionomers is almost the same for all the materials investigated in this study. The average total areas for the various families are also listed in Table 1. All of these observations, along with some of those in the previous paragraph, suggest that the volume fraction of the cluster phase for the acrylates is smaller than that for the methacrylates at the same ion content.

It is useful to inquire why in two such similar ionomers one finds different relative amounts of clustered material. The multiplet/cluster concept is most useful in this connection.[13] The only parameter which differs in the two materials is the nature of the ionic repeat units, i.e., acrylate vs methacrylate, and these, in turn, differ only in the presence of a methyl group on the $\alpha$-carbon of the ionic repeat unit. This methyl group affects the "contact surface area of the chain" which is defined as the area of the segments of the chain which are connected to the pendant ion and which cannot get out of the way when the multiplet is formed. They are thus in contact with the multiplet. Since the ion pairs are identical, the radius of the multiplet is inversely related to the contact surface area of the chain, as was discussed extensively in ref 12. This suggests that the multiplets in the acrylate system would be somewhat larger than those in the methacrylate system. It follows that the number of ion pairs per core as well as the size of the multiplets for the acrylates is marginally larger than that for the methacrylates. Thus, for the same ion content, there are fewer multiplets in the acrylates, and they are further apart.

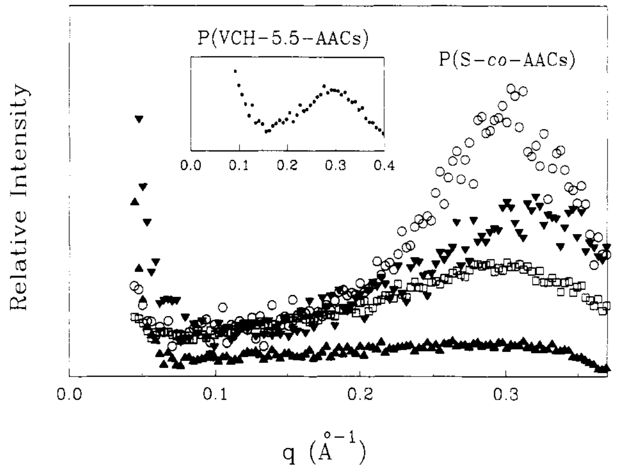

**Figure 6.** SAXS data for several P(S-*co*-AACs) ionomers. Symbols give the ion content in mole percent: ○ (24.7%), ▼ (17.3%), □ (11.6%), and ▲ (6.5%). The insert shows the data for the P(VCH-5.5-AACs) ionomer.

SAXS results, to be discussed below, are consistent with the possibility suggested above. Figure 6 shows the SAXS data for the P(S-*co*-AACs) systems, along with the SAXS profile of the P(VCH-5.5-AACs) ionomer. The positions of peak maxima at ca. $q$ = 0.30–0.31 Å$^{-1}$ are practically independent of the ion content. They also show a significant upturn in the small $q$ range. The Bragg spacings obtained from the ionic peak maxima ($d_{\text{Bragg}} = 2\pi/q_{\max}$) remain constant within experimental error ($d_{\text{Bragg}}$ = 22 ± 0.4 Å). To calculate the aggregation number of the ion pairs per core, it is assumed that the Bragg spacing arises from interparticle scattering related to the distance between multiplets, that the multiplets are uniformly distributed in the material that has a density of 1.04 g/cm$^3$, and that all ion pairs are in multiplets. For comparative purposes, we further assume a cubic lattice. All these assumptions may not hold in the present systems, but they allow us to obtain numbers needed to compare the behavior in the acrylates and methacrylates, since the assumptions made for both systems are identical. Using these assumptions, one finds that, in the P(S-10.0-AACs) system, there are 5.8 ion pairs per multiplet. By contrast, for the methacrylate ionomer containing 10 mol % of ions, the Bragg spacing is 20 ± 0.3 Å,[35] and the number of ion pairs per core is found to be 4.3 based on the same assumptions as above. This difference in the number of ion pairs per core arises from the presence of the methyl group of the methacrylate ionomers and its absence in the acrylates. It should be noted, however, that these small differences are subject to some experimental error.

It should be stressed that the persistence length of polystyrene in these two ionomer systems is, obviously, identical. As was pointed out in the previous publication,[23] the size of the multiplets exerts a strong influence on the total amount of clustered material. At the same ion content, it was shown that, in the styrene–styrenesulfonate ionomers, the number of ion pairs per core is larger than that in the styrene–methacrylates, and thus the size of the multiplet is larger, which implies that the total number of multiplets in the sample is smaller than in the styrene–methacrylate ionomers. Since the thickness of the restricted mobility layer which is on the order of the persistence length is the same in both, it means that the

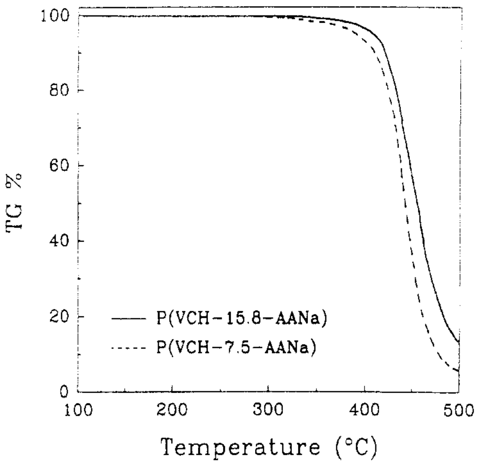

**Figure 7.** TGA thermograms for P(VCH-*co*-AANa) ionomers with ion contents of 7.5 (- - -) and 15.8 mol % (—).

total amount of material of restricted mobility is smaller in the styrene–styrene sulfonate [P(S-*co*-SS)] ionomers. It should be recalled that the volume of the shell of restricted mobility surrounding the multiplet is governed by the thickness of the restricted mobility layer, i.e., on the order of the persistence length. This is discussed extensively in ref 23. The same reasoning can be applied to explain the difference in the mechanical properties between the methacrylates and the acrylates. Since the methacrylate ionomers contain multiplets of a smaller size but in larger numbers than the acrylate ionomers, they are somewhat closer together. Thus, they contain a relatively higher volume fraction of material of restricted mobility, because the restricted mobility region will overlap more extensively. Therefore, for the methacrylates, there is more cluster material per ion pair, and the cluster $T_g$ and ionic plateau are higher than those for the acrylates.

In the flow region, it is seen that, for the sample containing ca. 6 mol % of ions, the loss tangent peak for the acrylate ionomer is less well developed than that for the methacrylates (see Figure 5). In the plots of the storage modulus, it is clear that for the acrylate ionomers the samples start to flow at lower temperatures than the methacrylates. Also, it should be pointed out that no rubbery plateau (at ca. $\log E' \sim 5.5$) is seen for the acrylate ionomers. The difference in behavior is due to the different molecular weights of the two polymers. Another study in this laboratory[36] showed that higher molecular weight ionomer exhibits a more well-developed cluster peak and rubbery modulus. In the present study, the number-average molecular weight of the methacrylates ($M_n \approx$ 500 000) was higher than that of the acrylate ionomers ($M_n \approx 100\,000$).

The activation energies of the cluster phase for the methacrylates, not shown here, are similar to those for the acrylates. However, for the methacrylates, the trends in the activation energies of the matrix phase vs ion content are somewhat different from those for the acrylates; this will be discussed in greater detail in a separate publication.[30]

**P(VCH-*co*-AANa) Ionomers.** Figure 7 shows the weight loss of two samples of different ion contents as a function of temperature. The temperatures of 1% and 5% weight loss for the P(VCH-7.5-AANa) sample are 310 and 390 °C, respectively, while those for the P(VCH-15.8-AANa) sample are 340 and 400 °C. Thus, in the present study, maximum temperatures of 310 and 340 °C, depending on the ion content, are suitable for the measurement of dynamic mechanical properties of these materials, since residence times are short.

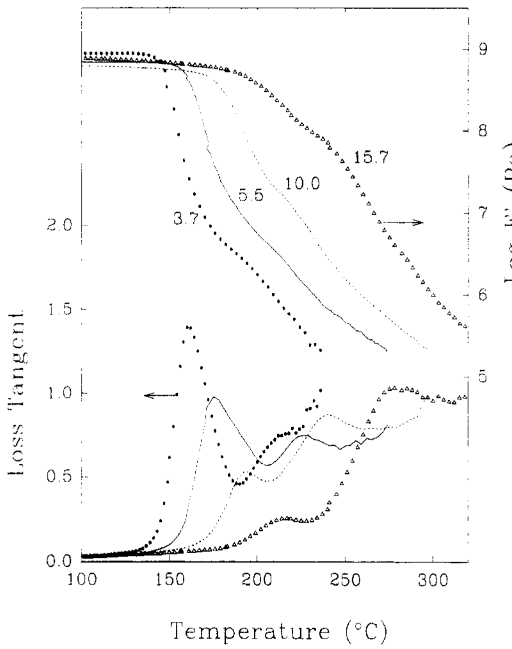

**Figure 8.** Storage moduli ($E'$) and loss tangents ($\tan \delta$) measured as a function of temperature at 1 Hz for several P(VCH-*co*-AANa) ionomers. The molar ion content is indicated for each sample.

Figure 8 shows a plot for a series of storage modulus and loss tangent curves for the P(VCH-*co*-AANa) ionomers of various ion contents as a function of temperature. As was observed in the polystyrene-based ionomers, there are two peaks in the plot of the loss tangent curves for all the ionomers. The materials which have a higher ion content, i.e., above 16 mol %, are very difficult to mold because of the very high cluster transition temperature. Again, curve resolution was applied to analyze the loss tangent peaks. The curve resolution results are also listed in Table 1; the transition temperatures are given in Figure 2. As in the other system, the peak temperatures increase with increasing ion content. The area under the matrix peak decreases with increasing ion content, while that for the cluster peak increases. From the storage modulus, it is seen that the ionic plateaus are not well developed.

As was mentioned before in connection with the polystyrene-based ionomers,[22,30] the widths at half-height of the loss tangent matrix peaks increase with increasing ion content and decrease for the cluster peaks. In those systems, at low ion content, the matrix phase is dominant and continuous, and the width at half-height for the matrix peak is narrow, while that for the cluster peak is broad. As the ion content increases, the cluster phase becomes dominant and probably even continuous. The peak width for the cluster transition narrows, while that for the matrix transition broadens with increasing ion content. It seems reasonable to suggest that the peak widths at half-height reflect the heterogeneity of the phases. In the P(VCH-*co*-AANa) system, Table 1 shows that the width at half-height of the matrix $\tan \delta$ peak increases slightly with increasing ion content. However, the cluster peak width at half-height also increases with increasing ion content. This trend is opposite to what was observed in the polystyrene-based ionomers, and no reasonable explanations come to mind for the behavior of the P(VCH-*co*-AA) system. The total area under the loss tangent peaks is almost the same as that in the other systems and, as in the styrene ionomers, remains independent of ion content. In addition, the activation energies for the transitions are in the same range as those for the polystyrene-based ionomers.

**Comparison P(VCH-*co*-AANa) Ionomers with P(S-*co*-AAna) Ionomers.** Figure 5b shows the loss tangent and storage modulus curves for the P(S-11.6-AANa) and P(VCH-11.8-AANa) samples. There are two tan $\delta$ peaks in both samples. The peak temperatures of the matrix and cluster transitions for the P(VCH-*co*-AANa) ionomers are much higher than those for the styrene-based ionomers. It is worth noting that the glass transition temperature of the homopoly(cyclohexylethylene) (i.e., vinylcyclohexane in this paper) is ca. 120 °C, while that for the polystyrene is ca. 100 °C determined by DSC.[29] As was suggested by Taylor and Davison,[37] this difference probably arises from the increased bulkiness of the cyclohexyl group relative to that of the phenyl ring. For the purpose of comparison of the relative volumes of these two groups, i.e., benzene and cyclohexane, one may use the densities in the liquid state at 20 °C and the molecular weights of benzene ($d$ = 0.879, MW = 78.11) and of cyclohexane ($d$ = 0.779, MW = 84.16)[38] and calculate the volumes per mole; they are 108 and 89 mL for cyclohexane and benzene, respectively. The more bulky pendant group, i.e., cyclohexane, increases the stiffness of the polymer chain and thus increases the $T_g$ of the material.

From Table 1, it is clear that at comparable ion contents the fractional area under the cluster peak is smaller for the vinylcyclohexane ionomers than that for the styrene-based ionomers (it should be stressed that all the ionomer samples were subjected to an identical thermal treatment). For instance, the fractional area under the cluster peak for the P(VCH-7.5-AANa) is 0.35, while that for the P(S-6.5-AANa) is 0.60. A possible explanation for this comes from a study of the styrene-*co*-4-vinylpyridinium system.[39] The random styrene-*co*-4-vinylpyridinium ionomers, in the unplasticized state, are unclustered, in contrast to those in the plasticized state. It was suggested that the reason for this behavior is the high matrix glass transition temperature. The addition of a nonpolar plasticizer to the copolymer lowers the glass transition temperature of the matrix sufficiently to induce extensive clustering. This suggests that, at or above the $T_g$ of the unplasticized material, the electrostatic interaction is not strong enough to induce clustering or even multiplet formation. A lowering of the $T_g$ makes electrostatic interaction stronger relative to $kT_g$ and thus allows increased multiplet formation and clustering. The same reasoning is applicable to explain the decreased clustering in the vinylcyclohexane ionomers relative to the styrene system at the same ion concentration. In the vinylcyclohexane ionomers, the matrix $T_g$ is higher than that in the styrene-based ionomers. However, the strength of the electrostatic interaction is the same for both systems, because the ion pairs are identical. Therefore, those ion pairs which just barely fail to form multiplets for energetic reasons in the vinylcyclohexane system will be able to do so in the polystyrene-based ionomers. Thus, it is not unreasonable that the polystyrene ionomers are more clustered than the vinylcyclohexane ionomers of comparable ion content.

The SAXS results of these samples suggest that the Bragg spacings are independent of the ion content and are seen at ca. 22 Å. One of the typical SAXS profiles is shown in Figure 6. This distance is identical with that for the P(S-*co*-AACs) system. The intergroup distances, which are marginally longer than the "loopback" distance, are dominant in determining intermultiplet distances and give rise to a most preferred spacing. The loopback distance is that chain length between neighboring ion pairs below which the neighboring ion pairs are likely to find themselves in the same multiplet. It is believed that this spacing reflects the position of the SAXS peak of the material.[13] The loopback distances in these two systems are almost identical, and thus it is not surprising that the Bragg spacings of these two systems due to the intermultiplet scattering centers should be similar.

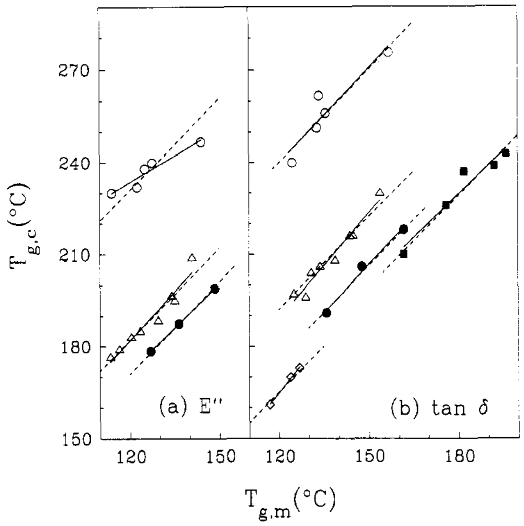

**Figure 9.** Cluster glass transition temperatures as a function of the matrix glass transition for the various ionomers which were determined from (a) $E''$ maxima and from (b) tan $\delta$ peaks at 1 Hz. Symbols ● and ■ represent the data for the P(S-*co*-AANa) and P(VCH-*co*-AANa) systems, respectively. Data for P(S-*co*-SSNa) (○) and P(S-*co*-SCNa) (◇) were obtained from ref 23 and those for P(S-*co*-MANa) (△) from ref 30. The solid lines indicate the linear regression lines, and the dashed lines indicate the best line with slope 1.

**Comparison of Matrix $T_g$ with Cluster $T_g$.** From Figure 5b, one finds that the difference in the two $T_g$s for the P(VCH-11.8-AANa) sample is almost the same as that for the P(S-11.6-AANa) sample. In addition, in Figure 2, the slopes of the regression lines are almost the same for all samples except the P(S-*co*-MANa) system. This means that the rates of the increase in the glass transition temperatures with ion content for all the samples are almost identical and suggests that the cluster and matrix $T_g$s experience a parallel increase with increasing ion content. To test this possibility, the matrix glass transition temperatures ($T_{g,m}$) are plotted against the cluster glass transition temperatures ($T_{g,c}$) in parts a and b of Figure 9. The values for the $T_g$s were obtained from loss modulus maxima (Figure 9a) as well as loss tangent peaks (Figure 9b) for the various ionomers. Only the data for samples in which both unclustered and clustered material is present to the extent of at least 15% (as determined from the areas under the peaks) are given in this figure. Samples with volume fractions less than that amount are not included, because atypical morphologies might be involved, if one of the two types of materials (clustered or unclustered) is present in very small quantities. This situation might be somewhat analogous to that in highly crystalline polymers in which the morphology of the amorphous phase can be very different, depending on the degree of crystallinity.[40,41] Thus, for the present data collection, in the P(S-*co*-MANa) system, the data[30] of the ionomers with ion content less than 2 mol % (area under the matrix tan $\delta$ peak > 85%) and higher than 10 mol % (area under the cluster tan $\delta$ peak > 85%) were eliminated. It should also be pointed out that, in the case of the P(VCH-*co*-AANa) and P(S-*co*-SCNa)[23] systems, the loss modulus curves show only one peak in the low-temperature range with a shoulder in the high-temperature range. Therefore, for the above two systems, the determination of the temperatures for

**Table 2. Regression Parameters in the Plots of $T_{g,m}$ vs $T_{g,c}$ for the Various Ionomer Systems**

| | solid line | | | dashed line (slope 1) | | | |
|---|---|---|---|---|---|---|---|
| ionomer | slope | intercept (°C) | $r^2$ | slope | intercept (°C)[a] | standard error (°C)[b] | $d_{\mathrm{Bragg}}$ (Å) at ~7 mol % |
| | | | | From tan $\delta$ Plots | | | |
| P(S-*co*-SSNa) | 1.01 | 118 | 0.932 | 1.00 | 120 | 2.1 | ~36[c] |
| P(S-*co*-MANa) | 1.05 | 63 | 0.947 | 1.00 | 72 | 0.9 | ~20[d] |
| P(S-*co*-AANa) | 1.03 | 51 | 0.994 | 1.00 | 56 | 0.9 | ~22 |
| P(VCH-*co*-AANa) | 0.95 | 58 | 0.969 | 1.00 | 49 | 1.5 | ~22 |
| P(S-*co*-SCNa) | 1.22 | 19 | 0.999 | 1.00 | 45 | 0.7 | ~30[c] |
| | | | | From $E''$ Plots | | | |
| P(S-*co*-SSNa) | 0.59 | 163 | 0.955 | 1.00 | 111 | 2.2 | ~36[c] |
| P(S-*co*-MANa) | 1.11 | 48 | 0.963 | 1.00 | 62 | 0.9 | ~20[d] |
| P(S-*co*-AANa) | 0.95 | 57 | 1.000 | 1.00 | 51 | 0.3 | ~22 |

[a] Listed in order of decreasing intercept of the dashed line. [b] Standard errors derived from the errors in the intercept. [c] Unpublished data from this lab. [d] Data from ref 30.

the cluster transitions was very difficult, and the data are not included here.

The slopes of the linear regression lines (solid lines) for the each ionomer were in the range of 0.95–1.22 from the data of loss tangent peaks and 0.59–1.11 from the loss modulus peaks. The dashed lines indicate the best lines with slope 1. The slopes, vertical intercepts, and regression coefficients for the solid line and standard error in the intercepts of the dashed lines are listed in Table 2. The slope of 1 means that the $T_g$s of both phases increase at the same rate. It should be stressed that two phases, i.e., the matrix and cluster phases, which have their own glass transition temperatures, are basically the same material. The only the difference between these two phases is the concentration of multiplets, and the degree of overlap of regions of restricted mobility surrounding the multiplets. Thus, it is not surprising that, with increasing ion content, the glass transition temperatures of the matrix phase increase by as much as those for the clustered regions. However, it should be mentioned that the number of data points is not high enough to collect extensive statistics. It should also be noted that while the slope of the linear regression line for the $E''$ peaks of the P(S-*co*-SSNa)[23] system was 0.59, only two points deviated substantially from the line of slope 1. This is, however, the only exception from an otherwise clear slope 1 pattern.

It is also of interest to explore the values of the vertical intercepts of the dashed lines, which represent the differences in the two $T_g$s. In Table 2, one can find data for two families of ionomers, i.e., one based on the sulfonates and the other on the carboxylates. The vertical intercepts for the sulfonates are much higher than those for the carboxylates. This is undoubtedly due to the increased interaction strengths of the sulfonates relative to the carboxylates. As was shown in a previous publication,[23] ion pair interchange is involved in the glass transition of the cluster phase of the styrene-based ionomers. Since the sulfonates are subject to much stronger interaction, bond interchange does not become an important factor until much higher temperatures are reached than in the corresponding carboxylates. Therefore, it is to be expected that the cluster glass transitions for the sulfonates should be very much higher.

The vertical intercepts in the carboxylates show a very interesting trend, decreasing from P(S-*co*-MANa) (72 °C), to P(S-*co*-AANa) (56 °C), to P(VCH-*co*-AANa) (49 °C), and to P(S-*co*-SCNa) (45 °C). It is of particular interest to note that the Bragg distances for the ionomer of ca. 7 mol % ion content showed an opposite trend. The relationship between these two trends is evident on brief consideration. The larger the Bragg distance, the larger the multiplet for the same ion content. While the Bragg distance is related to the intermultiplet spacing, one can calculate the size of the multiplets from space-filling considerations, if one assumes a lattice (cubic in this case). However, the larger the multiplet, the smaller the amount of the clustered material at the same ion concentration.[13,23] The smaller the amount of the clustered material, the less well developed the clusters will be, and the lower the glass transition temperature will be. Therefore, the difference in the two $T_g$s decreases with increasing size of the multiplets. It is worth noting that the trend of this type is what one expects on the basis of the recently proposed multiplet/cluster (EHM) model for the morphology of random ionomers.[13]

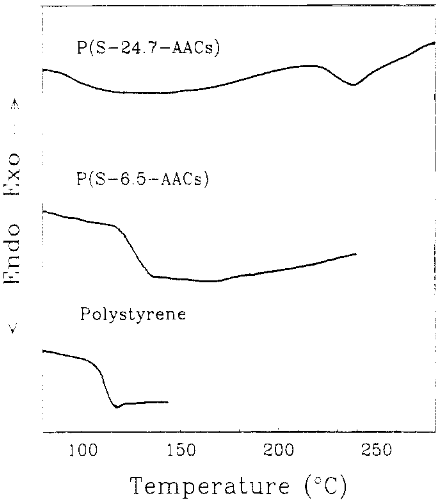

**Figure 10.** DSC thermograms for the polystyrene and P(S-*co*-AACs) ionomers with ion contents of 6.5 and 24.7 mol %.

**DSC.** Figure 10 shows the DSC thermograms of the three selected samples. The curve for polystyrene shows a $T_g$ at 111 °C, while that for P(S-24.7-AACs) shows it at 230 °C. As was pointed out before, in the case of the P(S-24.7-AACs) sample, the glass transition arises from the cluster phase. In the case of the P(S-6.5-AACs) system, the $T_g$ for the matrix phase is seen clearly but that for the cluster phase is not seen. This may be due to the small heat capacity change for the glass transition of the cluster phase. For the high ion content ionomers, i.e., above 11 mol % of ions, only one glass transition temperature per sample was observed using DSC, which is related to the cluster phase of the ionomers. Suchocka-Gałaś[42,43] also found one glass transition curve on DSC thermograms for the P(S-*co*-AANa) ionomers, and our results are in agreement. In the present study, for all the P(VCH-*co*-AANa) ionomers, again only one transition was observed in the DSC thermograms (not shown). These transition temperatures are very close to the matrix transition temperature obtained using the DMTA. This is very different behavior from the polystyrene-*co*-acrylate ion-

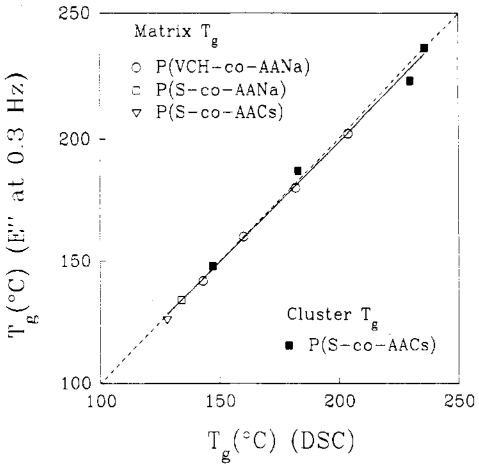

**Figure 11.** Glass transition temperatures obtained from the $E''$ peak maxima at 0.3 Hz as a function of those obtained from DSC. Open symbols indicate the matrix $T_g$, and filled symbols indicate the cluster $T_g$s. The solid line indicates the linear regression line, and the dashed line indicates the best line with a slope of 1.

omers in which the DSC detected the dominant transition due to either the matrix or the cluster glass transition.

Figure 11 compares the $T_g$s obtained by DSC with those determined using the DMTA for all the systems. For this comparison, the DMTA data from the temperatures of the loss modulus ($E''$) maxima at 0.3 Hz were used since these gave the best correlation. This figure shows an unambiguous linear relationship between the $T_g$s obtained from DSC and from DMTA, the same relationship holding for both cluster and matrix $T_g$s. Lee et al. also found similar results in the MDI-based polyurethane ionomer system.[44] It is noteworthy that while the loss tangent plots for the samples of intermediate ion content show two peaks reflecting respectively the two glass transitions of the matrix and cluster regions, the $E''$ plots show only a single maximum reflecting either the matrix or the cluster transitions; very frequently, however, a second shoulder appears on the $E''$ plot instead of a fully developed peak. The assignment is unambiguous from the comparison of the loss tangent and $E''$ plots. For those materials in which only a single peak appears in the $E''$ curve (and this is the case for both systems studied here) only a single $T_g$ is observable in DSC curves also.

## Conclusions

This study describes an investigation of the effects of the chemical structure of random ionic copolymers on their mechanical properties. Two series of acrylate ionomers based on styrene and vinylcyclohexane were synthesized, with ion contents up to 30 and 16 mol %, respectively. The general trends in the mechanical properties of the styrene–acrylate ionomers are the same as those of the styrene–methacrylates. Both the matrix and cluster glass transition temperatures increase with increasing ion content. The peak width at half-height of the matrix tan $\delta$ peak increases, while that of the cluster peak decreases with increasing ion content. In the case of P(S-29.6-AACs), which contains only clustered material, the shape of the storage modulus curve and the value of the activation energy for the glass transition is similar to that for nonionic polystyrene which contains only the matrix phase. This further reinforces the identification of the cluster peak (tan $\delta$ or $E''$) as a glass transition.

A comparison of the mechanical properties of the styrene-based acrylates and methacrylates illustrates the effects of the presence of the methyl group on the $\alpha$-carbon of the methacrylates. The matrix $T_g$s are the same for both systems, but for the methacrylates the cluster $T_g$s are higher than those for the acrylates. This also results in a higher and longer ionic plateau in the methacrylates than in the acrylates. The difference in properties arises from the differences in the contact surface area of the chain which is bigger for the methacrylates (due to the presence of the methyl group) than for the acrylates. It follows that the methacrylates form smaller multiplets but in larger numbers than the acrylates. Thus, they contain a relatively higher volume fraction of clustered materials than the acrylates. SAXS confirms that in the methacrylates the number of ion pairs per ionic core is smaller than that in the acrylates.

In the case of the vinylcyclohexane ionomers, two peaks are seen in the loss tangent plot and in the storage modulus plots; however, the ionic plateau is not as well developed as in the styrene ionomers. A comparison of the vinylcyclohexane–acrylates and styrene–acrylates illustrates the effect of the bulkiness of the pendant group on the mechanical properties of the materials. Both the matrix and cluster $T_g$s are higher for the vinylcyclohexane-based ionomers than for the styrene-based ionomers. This is due to the bulkiness of the pendant cyclohexyl group, which increases the stiffness of the chain relative to that of polystyrene. Also, because of the higher matrix $T_g$, the vinylcyclohexane ionomers contain fewer ions in the multiplets (and a smaller percentage of ions in multiplets) than the styrene-based ionomers. Thus, at the same ion content, the volume fraction of clustered materials in the vinylcyclohexane ionomers is smaller than that in the styrene-based ionomers.

For all samples in this study, the cluster and matrix $T_g$s show a parallel increase with increasing ion contents. This is reasonable, because the material in two phases, i.e., the cluster and matrix phases, is basically the same. The difference in the two $T_g$s increases with increasing strength of the ion interaction and decreases with increasing size of the multiplet.

For all samples, DSC thermograms show only one glass transition which corresponds to either that of the matrix or that of the cluster. The relationship between the $T_g$s obtained from DSC and those from loss modulus peaks (at 0.3 Hz) shows excellent linearity. Even though the loss tangent plots show two peaks, the $E''$ plots show only a single maximum. For those materials in which only a single peak is present in the $E''$ curve, only a single $T_g$ is observable in DSC curves.

**Acknowledgment.** The assistance of Dr. Claudine E. Williams in the acquisition of the X-ray data at LURE is gratefully acknowledged. The authors are also indebted to the PPRIC for the use of the SAXS camera. This work was supported, in part, be a grant from NSERC Canada.

## References and Notes

(1) Holliday, L., Ed. *Ionic Polymers*; Applied Science Publishers: London, 1975.

(2) Eisenberg, A.; King, M. *Ion-Containing Polymers, Physical Properties and Structure*; Academic Press: New York, 1977.

(3) Eisenberg, A., Ed. *Ions in Polymers*; Advances in Chemistry Series 187; American Chemical Society: Washington, DC, 1980.

(4) MacKnight, W. J.; Earnest, T. R., Jr. *J. Polym. Sci., Macromol. Rev.* **1981**, *16*, 41.

(5) Eisenberg, A., Bailey, F. E., Eds. *Coulombic Interactions in Macromolecular Systems*; ACS Symposium Series 302; American Chemical Society: Washington, DC, 1986.

(6) Pineri, M., Eisenberg, A., Eds. *Structure and Properties of Ionomers*; NATO Advanced Study Institute Series 198; D. Reidel Publishing Co.: Dordrecht, Holland, 1987.

(7) Tant, M. R.; Wilkes, G. L. *J. Macromol. Sci., Rev. Macromol. Chem. Phys.* **1988**, *C28*, 1.

(8) Mauritz, K. A. *J. Macromol. Sci., Rev. Macromol. Chem. Phys.* **1988**, *C28*, 65.

(9) Fitzgerald, J. J.; Weiss, R. A. *J. Macromol. Sci., Rev. Macromol. Chem. Phys.* **1988**, *C28*, 99.

(10) Utracki, L. A.; Weiss, R. A., Eds. *Multiphase Polymers: Blends and Ionomers*; ACS Symposium Series 395; American Chemical Society: Washington, DC, 1989.

(11) Lantman, C. W.; MacKnight, W. J.; Lundberg, R. D. In *Comprehensive Polymer Science*; Allen, G., Bevington, J. C., Eds.; Pergamon Press: Oxford, U.K., 1989; Vol. 2, Chapter 25.

(12) Eisenberg, A. *Macromolecules* **1970**, *3*, 147.

(13) Eisenberg, A.; Hird, B.; Moore, R. B. *Macromolecules* **1990**, *23*, 4098.

(14) Lundberg, R. D.; Makowski, H. S. In *Ions in Polymers*; Eisenberg, A., Ed.; Advances in Chemistry Series 187; American Chemical Society: Washington, DC, 1980.

(15) Rigdahl, M.; Eisenberg, A. *J. Polym. Sci., Polym. Phys. Ed.* **1981**, *19*, 1641.

(16) Visser, S. A.; Cooper, S. L. *Macromolecules* **1991**, *24*, 2576.

(17) Venkateshwaran, L. N.; Tant, M. R.; Wilkes, G. L.; Carlier, P.; Jérôme, R. *Macromolecules* **1992**, *25*, 2996.

(18) Sanui, K.; Lenz, R. W.; MacKnight, W. J. *J. Polym. Sci., Polym. Chem. Ed.* **1974**, *12*, 1965.

(19) Azuma, C.; MacKnight, W. J. *J. Polym. Sci., Polym. Chem. Ed* **1977**, *15*, 547.

(20) Rahring, D.; Azuma, C.; MacKnight, W. J. *J. Polym. Sci., Polym. Phys. Ed.* **1978**, *16*, 59.

(21) Rahring, D.; MacKnight, W. J. In *Ions in Polymers*; Eisenberg, A., Ed.; Advances in Chemistry Series 187; American Chemical Society: Washington, DC, 1980; Chapters 6 and 7.

(22) Hird, B.; Eisenberg, A. *J. Polym. Sci., Polym. Phys. Ed.* **1990**, *28*, 1655.

(23) Hird, B.; Eisenberg, A. *Macromolecules* **1992**, *25*, 6466.

(24) Gauthier, M.; Eisenberg, A. *Macromolecules* **1990**, *23*, 2066.

(25) Moore, R. B.; Bittencourt, D.; Gauthier, M.; Williams, C. E.; Eisenberg, A. *Macromolecules* **1991**, *24*, 1376.

(26) Clas, S. D.; Eisenberg, A. *J. Polym. Sci., Polym. Phys. Ed.* **1986**, *24*, 2767.

(27) Wilson, A. D., Prosser, H. J., Eds. *Developments in Ionic Polymers-1*; Applied Science Publishers: London, 1983.

(28) Eisenberg, A., Yeager, H. L., Eds. *Perfluorinated Ionomer Membranes*; ACS Symposium Series 180; American Chemical Society: Washington, DC, 1982.

(29) Brandrup, J., Immergut, E. H., Eds. *Polymer Handbook*; John Wiley & Sons: New York, 1988.

(30) Kim, J.-S.; Jackman, R. J.; Eisenberg, A., to be published.

(31) Osada, M.; Nakazawa, M. Jpn Patent 01 062 307, 1989.

(32) Mark, H. F., Othmer, D. F., Overberger, C. G., Seaborg, G. T., Eds. *Encyclopedia of Chemical Technology*, A Wiley-Interscience Publication; John Wiley & Sons: New York, 1979.

(33) Perrin, D. D., Armarego, W. L. F., Eds. *Purification of Laboratory Chemicals*, 3rd ed.; Pergamon Press: Oxford, U.K., 1988.

(34) Macintyre, J. E., Ed. *Dictionary of Inorganic Compounds*; Chapman & Hall: London, 1992; Vol. 3.

(35) Jiang, M.; Gronowski, A. A.; Yeager, H. L.; Wu, G.; Kim, J.-S.; Eisenberg, A., to be published.

(36) Kim, J.-S.; Yoshikawa, K.; Eisenberg, A., to be published.

(37) Taylor, G. L.; Davison, S. *J. Polym. Sci., Part B* **1968**, *6*, 699.

(38) Weast, R. C., Lide, D. R., Astle, M. J., Beyer, W. H., Eds. *CRC Handbook of Chemistry and Physics*, 70th ed.; CRC Press: Boca Raton, FL, 1989.

(39) Wollmann, D.; Williams, C. E.; Eisenberg, A. *Macromolecules* **1992**, *25*, 6775.

(40) Boyer, R. F. *Macromolecules* **1973**, *6*, 288.

(41) Boyer, R. F. *J. Macromol. Sci.* **1973**, *B8*, 503.

(42) Suchocka-Gałaś, K. *Eur. Polym. J.* **1989**, *25*, 1291.

(43) Suchocka-Gałaś, K. *Eur. Polym. J.* **1990**, *26*, 1203.

(44) Lee, D.-c.; Register, R. A.; Yang, C.-z.; Cooper, S. L. *Macromolecules* **1988**, *21*, 1005.